

Cite this: *Chem. Sci.*, 2022, 13, 2729 All publication charges for this article have been paid for by the Royal Society of Chemistry

Received 4th November 2021

Accepted 9th February 2022

DOI: 10.1039/d1sc06135f

rsc.li/chemical-science

Atropenantioselective palladaelectro-catalyzed anilide C–H olefinations viable with natural sunlight as sustainable power source†

Johanna Frey,  ‡^a Xiaoyan Hou,  ‡^a and Lutz Ackermann  *^{ab}

Enantioselective electrocatalyzed transformations represent a major challenge. We herein achieved atropenantioselective pallada-electrocatalyzed C–H olefinations and C–H allylations with high efficacy and enantioselectivity under exceedingly mild reaction conditions. With (*S*)-5-oxoproline as the chiral ligand, activated and non-activated olefins were suitable substrates for the electro-C–H activations. Dual catalysis was devised in terms of electro-C–H olefination, along with catalytic hydrogenation. Challenging enantiomerically-enriched chiral anilide scaffolds were thereby obtained with high levels of enantio-control in the absence of toxic and cost-intensive silver salts. The resource-economy of the transformation was even improved by directly employing renewable solar energy.

Introduction

Organic electrochemistry has recently emerged as a transformative platform in molecular syntheses,¹ enabling the use of electrons as sustainable redox reagents within electron-catalysis manifolds.² Regio- and chemo-selective transformations have thus been accomplished by dialling in the appropriate electrolysis potential. However, despite recent advances in asymmetric electrochemistry,³ enantioselective electrocatalysis continues to be scarce. This can be ascribed to key challenges, such as electrochemical degradation of the catalyst or of the chiral ligand, while unfavourable interactions of the electrolyte within the enantio-determining transition state need to be fully controlled to achieve full selectivity control.

Chiral axis represent key scaffolds in natural products, biologically active compounds, chiral ligands and functional materials.⁴ Particularly, biaryls are omnipresent and their syntheses have been accomplished by means of cross-coupling, arene assembly and the functionalization of racemic or pro-chiral biaryls, among others.⁵ In sharp contrast, the asymmetric assembly of molecules bearing an acyclic anilide motif with axial chirality has arguably received significantly less attention.⁶ As this structural moiety has a greater degree of rotational freedom than have biaryls, the control of the enantioselectivity

is considerably more difficult. Thus, exceedingly mild reaction conditions are required to ensure effective chiral induction, as well as to warrant the atropostability of the thus-obtained products. In this regard, Curran and Taguchi have made pioneering contributions towards the efficient catalytic asymmetric synthesis of such compounds.⁷ The efficiency of the enantioinduction was improved by *inter alia* nitrogen-functionalizations,⁸ cycloadditions for arene construction,⁹ organocatalytic nucleophilic additions¹⁰ or C–H functionalizations by dynamic kinetic resolution, with major advances by Shi.¹¹ Contrasting with this indisputable progress, these strategies suffer from the use of prefunctionalized substrates or – in the latter case of C–H activations – from stoichiometric amounts of expensive and toxic strong silver(I) chemical oxidants, giving rise to undesirable by-products in stoichiometric quantities. This significantly compromises the resource-economy of the overall strategy.¹²

In this context, we very recently reported on the asymmetric metalla-electrocatalyzed C–H activation enabled by a transient directing group, that is through substrate controlled selectivity.¹³ In sharp contrast, we have now developed a strategy for asymmetric electrocatalysis *via* electro-catalyst control to access synthetically-meaningful axially-chiral anilides by electro-oxidative palladium(II)-catalyzed C–H activation (Fig. 1). Hence, dynamic kinetic resolution provided access to a wide range of chiral anilides with a readily available and inexpensive chiral ligand, featuring outstanding levels of resource-economy, electricity as the sacrificial oxidant, and molecular hydrogen as the only by-product.

Results and discussion

Optimisation

We initiated our studies by probing the enantioselective C–H olefination of *N*-benzyl-*N*-(2-isopropylphenyl)picolinamide (**1a**)

^aInstitut für Organische und Biomolekulare Chemie, Georg-August-Universität Göttingen, Tammannstraße, 237077 Göttingen, Germany. E-mail: Lutz.Ackermann@chemie.uni-goettingen.de; Web: <http://www.ackermann.chemie.uni-goettingen.de/>

^bWöhler Research Institute for Sustainable Chemistry, Georg-August-Universität Göttingen, Tammannstraße 2, 37077 Göttingen, Germany

† Electronic supplementary information (ESI) available. See DOI: 10.1039/d1sc06135f

‡ These authors contributed equally to this work.



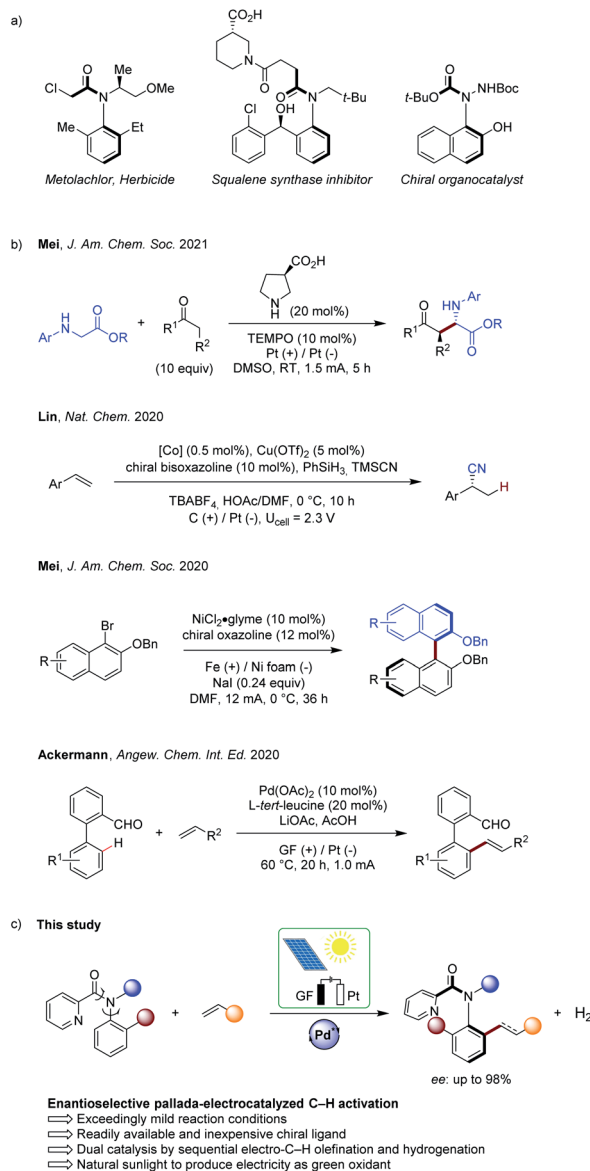


Fig. 1 (a) Examples of chiral anilides in crop protection, pharmaceuticals and asymmetric synthesis. (b) Recent examples of asymmetric organic electrocatalysis. (c) Enantioselective electro-catalyzed C-H activation to access chiral anilides by electrochemistry.

with *tert*-butyl acrylate (**2a**). We were pleased to note that under a 4.0 mA constant current electrolysis (CCE), the expected product **3aa** could be isolated in 11% yield and with 78% ee (Table 1, entry 2).¹⁴ The use of catalytic amounts of the redox-mediator¹⁵ 1,4-benzoquinone (BQ) proved to be beneficial to improve the efficacy, to give the product **3aa** in 78% yield and with 97% ee (entries 3–6), which is likely due to a stabilization of palladium(0) species. The catalysis was efficient both under air or under a nitrogen atmosphere (entries 3 and 7). Addition of an electrolyte did not affect the reaction outcome (entry 8). At 60 °C, the enantioselectivity of the reaction remained unchanged (entry 1). However, a slight decrease in enantioselectivity was found at an elevated temperature of 70 °C and an increased current of 6 mA (entry 9). At 60 °C, increasing the

Table 1 Optimization of the atroposelective electrocatalyzed C–H olefination^a

Reaction conditions: Pd(OAc)₂ (10 mol%), GF/Pt, L-4 (20 mol%), 1,4-BQ (10 mol%), NaOAc (2 equiv), TFE/DME, 24 h, 60 °C, CCE @ 4.0 mA

Entry	Deviation from standard conditions	Yield [%]	ee [%]
1	No deviation	90	98
2	50 °C, no 1,4-BQ	11	78
3	50 °C	78	97
4	50 °C, Cu(OAc) ₂ ·H ₂ O instead of 1,4-BQ	32	76
5	50 °C, (4-BrC ₆ H ₄) ₃ N instead of 1,4-BQ	22	86
6	50 °C, ferrocene instead of 1,4-BQ	57	96
7	50 °C, under N ₂ atmosphere	65	98
8	50 °C, adding <i>n</i> -Bu ₄ NPF ₆ (2 equiv.)	60	98
9	70 °C, 6 mA instead of 4 mA	70	96
10	6 mA instead of 4 mA	88	97
11	2 mA instead of 4 mA	51	98
12	Divided cell setup	45	95
13	CPE ^b @ 0.8 V	63	96
14	CPE ^b @ 0.4 V	81	97

^a Reaction conditions: undivided cell, **1a** (0.5 mmol), **2a** (1.5 mmol), [Pd] (10 mol%), **L-4** (20 mol%), 1,4-BQ (10 mol%), NaOAc (1.0 mmol), 2,2,2-trifluoroethanol (2.5 mL), DME (2.5 mL), 24 h, graphite felt (GF) anode, Pt-plate cathode, isolated yields. ^b Constant anodic potential with a silver as the reference electrode.

current to 6 mA did not alter the asymmetric olefination (entry 10), yet a lower current decreased the yield significantly (entry 11).

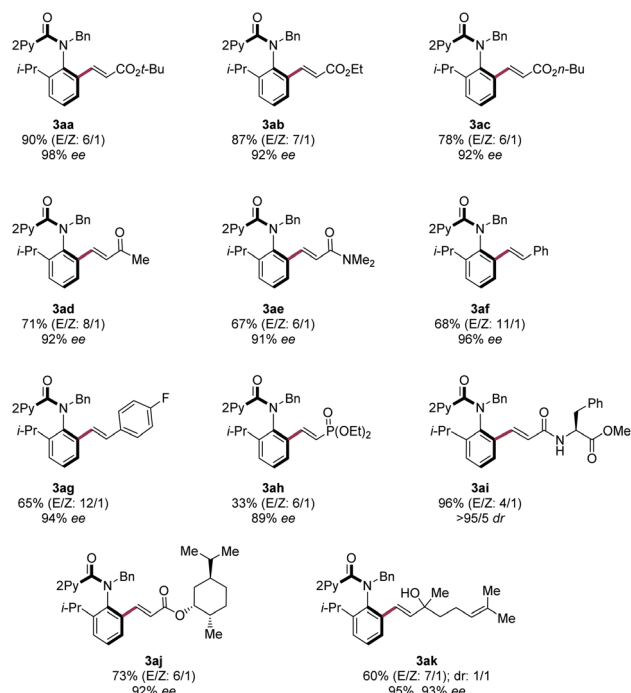
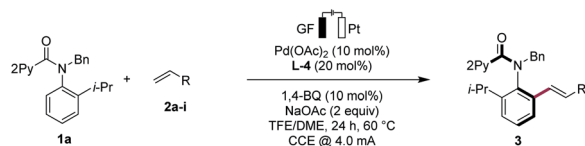
The efficiency of the electrocatalysis dropped when using a divided cell setup (entry 12). Finally, we noted that the reaction also proceeded in a constant potential electrolysis (CPE) mode and a high efficiency and very good enantioselectivity was observed at 0.4 V (entries 13 and 14). Control experiments confirmed the essential role of the electricity and the palladium catalyst.¹⁴

Robustness

With the optimized electrocatalysis conditions in hand, we next studied the scope of the atropoenantioselective C–H olefination of anilides **1** (Scheme 1). First, we explored the reaction of different olefinic partners **2**. Various acrylates **2a–2c** proved thereby amenable to obtain products **3** with excellent enantioselectivities. Vinyl-ketones **2d** and tertiary or secondary amides **2e** and **2i** were well-tolerated, as were styrenes **2f** and **2g**. Fluorinated styrene **2g** allowed to access the expected product **3ag** in 65% yield and with 94% ee. Vinyl phosphonates **2h** could successfully be used likewise. Olefins derived from natural products, such as menthol (**2j**) or linalool (**2k**), were also very well-tolerated.

Second, challenging allylations were probed, starting from non-activated alkenes **2l** and **2m**. Thereby, products **3al** and

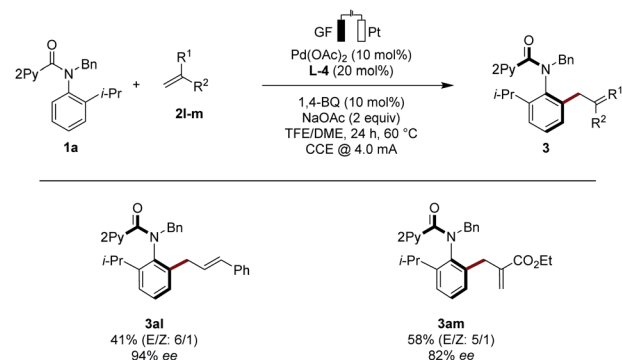




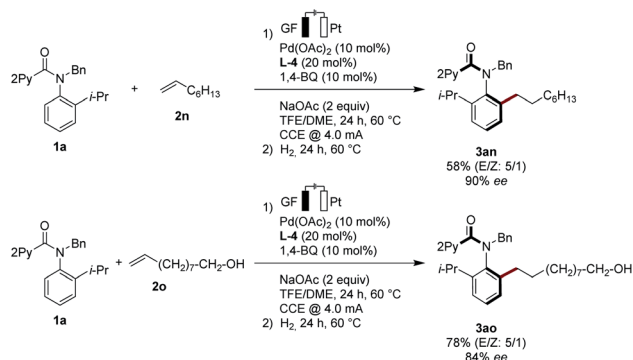
Scheme 1 Scope of the reaction regarding the olefin partner.

3am were obtained respectively, reflecting the robust scope of the pallada-electrocatalysis (Scheme 2).

Non-activated alkenes 1-octene (**2n**) and 9-decen-1-ol (**2o**) were also identified as suitable substrates for the enantioselective pallada-electrocatalysis. Here, subsequent stirring of the electrocatalysis mixture under an atmosphere of hydrogen provided access to the alkylated products **3an** and **3ao** with high enantioselectivities (Scheme 3). The mild nature of the



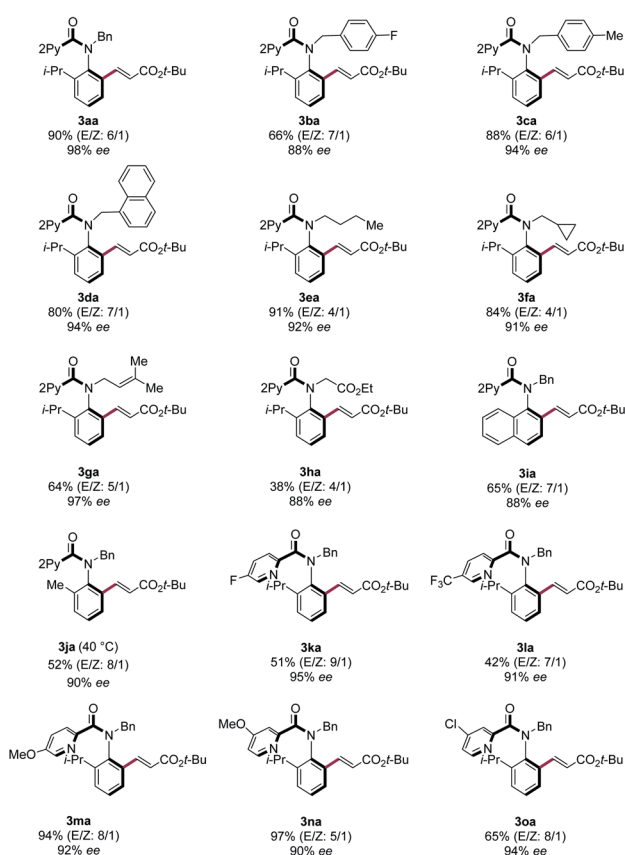
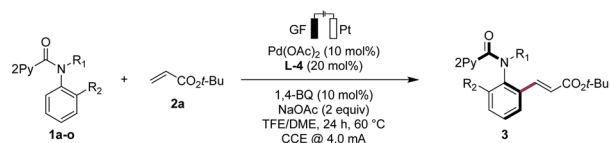
Scheme 2 Atropoenantioselective C-H allylation by electrochemistry.



Scheme 3 Dual electrocatalysis and hydrogenation manifold.

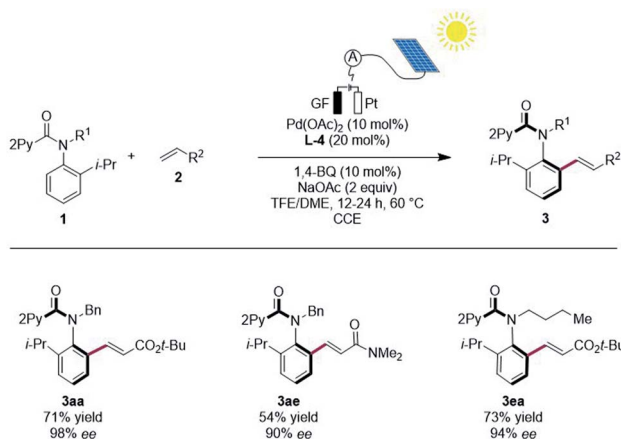
palladaelectro-catalyzed C-H functionalization was reflected by the full tolerance of the free hydroxyl group in substrate **2o**.

Third, various *N*-substituted anilides **1b-h** were tested in the electrocatalytic asymmetric C-H olefination. Replacing the isopropyl *ortho*-substituent by a naphthyl group gave the



Scheme 4 Scope of the reaction regarding the anilide partner.





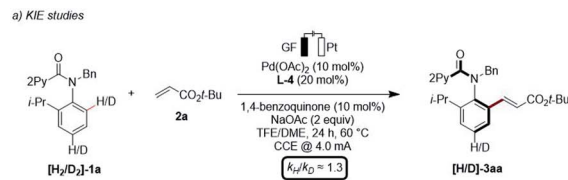
Scheme 5 Renewable solar energy for atroposelective C–H olefinations.

desired product **3ia** in 65% yield and 88% ee, while a methyl group led to a slight decrease in the enantioselectivity. However, by lowering the electrocatalysis temperature to 40 °C, we achieved a high enantioselectivity. Both electron-donating and electron-withdrawing groups were well tolerated on the pyridine motif, as was evidenced by the successful use of the anilides **1k–o** (Scheme 4).

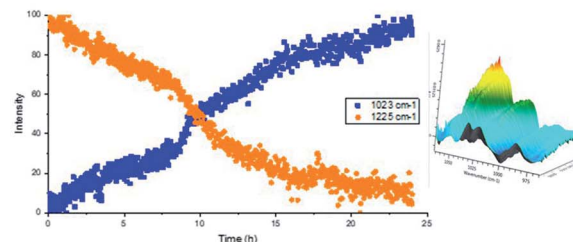
To significantly improve the resource-economy¹² of our strategy, we next performed the constant current electrolysis solely powered by renewable energy.¹⁶ To this end, we employed commercially available photovoltaic cells as the only power supply, guaranteeing high activity and enantioselectivity, when directly using natural sunlight (Scheme 5).

Mechanistic studies

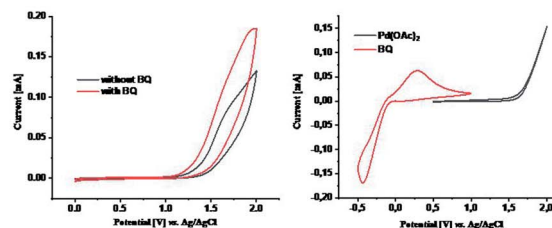
Finally, we became interested in unravelling the mode of action of the asymmetric pallada-electrocatalysis. Given that bimetallic Pd–Ag or Ag–Ag species have previously been suggested to facilitate the C–H activations,¹⁷ we hypothesized whether electrocatalysis would not only improve the sustainability, but also change the nature of the rate-determining step. In line with this hypothesis, a kinetic isotope effect (KIE) of $k_{\text{H}}/k_{\text{D}} \approx 1.3$ was suggestive of a fast C–H metalation step (Scheme 6a),¹⁴ contrasting with a KIE of 2.3 when employing silver(i) oxidants.^{11b} Qualitative *in operando* infrared spectroscopy allowed us to unravel a short induction period (Scheme 6b).¹⁴ Furthermore, we performed detailed studies by means of cyclic voltammetry (Scheme 6c).¹⁴ Thus, we observed a decrease of the onset oxidation potential in the presence of BQ, indicating its beneficial effect on the anodic oxidation. Thus, the BQ is proposed to serve a dual role, namely as a redox mediator as well as a ligand to stabilize palladium(0) species. A current dependence was next explored within a range from 1.0 to 6.0 mA (Scheme 6d). These findings were indicative of the electron transfer step being the rate limiting step, with a plateau being reached above 4.0 mA.



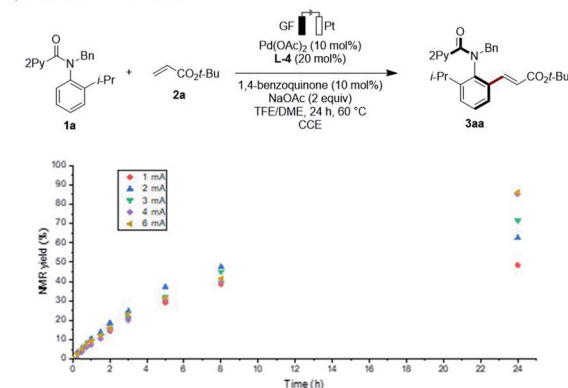
b) *In operando* React-IR: Plot of the observed vibrations over time and 3D-surface plot of the vibration at 1023 cm^{-1}



c) Cyclic voltammetry of the mixture of **1a**, **2a**, Pd(OAc)₂, L-4 and NaOAc, with and without 1,4-BQ (on the left) and of Pd(OAc)₂ and 1,4-benzoquinone separately (on the right)



d) Kinetic studies at different current



Scheme 6 Key mechanistic experiments. Cyclic voltammetry measurements were recorded in TFE/DME (1/1) at a substrate concentration of 5.0 mM and with 0.1 M *n*-Bu₄NPF₆ as supporting electrolyte. The scan rate is 100 mV s^{-1} .¹⁴

Conclusions

We have reported on unprecedented catalyst-controlled atroposelective pallada-electrocatalyzed C–H activations, which provide access to synthetically-meaningful chiral anilides without stoichiometric amount of chemical oxidants. 1,4-Benzoquinone was identified as the catalytic redox-mediator of choice, with molecular hydrogen as the only stoichiometric by-product. Thereby, an electrochemical degradation of the palladium catalyst could be avoided with sodium acetate as additive, serving both as a base and as an electrolyte without altering the enantioselectivity. Overall, we accessed enantioenriched



anilides with high levels of enantioselectivity under exceedingly mild reaction conditions. Dual catalysis proved to be likewise viable, allowing electrocatalyzed C–H olefination, along with subsequent hydrogenation. The asymmetric electrocatalysis employed electricity as a sustainable oxidant, and could even be carried out using a commercial solar panel with natural sunlight as the sole power source.

Data availability

All experimental data, procedures for data analysis and pertinent data sets are provided in the ESI.†

Author contributions

J. F. and L. A. conceived the project, J. F. and X. H. performed the experiments, X. H. performed CV studies. J. F. and L. A. wrote the manuscript.

Conflicts of interest

There are no conflicts to declare.

Acknowledgements

Generous support by the ERC Advanced Grant no. 101021358 (conferred on L. A.), DFG (Gottfried-Wilhelm-Leibniz award to L. A.) and the CSC (PhD fellowship to X. H.) is gratefully acknowledged.

Notes and references

- For representative reviews on organic electrochemistry, see: (a) L. F. T. Novaes, J. Liu, Y. Shen, L. Lu, J. M. Meinhardt and S. Lin, *Chem. Soc. Rev.*, 2021, **50**, 7941–8002; (b) C. Ma, P. Fang, D. Liu, K.-J. Jiao, P.-S. Gao, H. Qiu and T.-S. Mei, *Chem. Sci.*, 2021, **12**, 12866–12873; (c) P. Gandeepan, L. H. Finger, T. H. Meyer and L. Ackermann, *Chem. Soc. Rev.*, 2020, **49**, 4254–4272; (d) Y.-K. Xing, Q.-L. Yang, H. Qiu and T.-S. Mei, *Acc. Chem. Res.*, 2020, **53**, 300–310; (e) J. C. Siu, N. Fu and S. Lin, *Acc. Chem. Res.*, 2020, **53**, 547–560; (f) T. H. Meyer, I. Choi, C. Tian and L. Ackermann, *Chem*, 2020, **6**, 2484–2496; (g) P. Wang, X. Gao, P. Huang and A. Lei, *ChemCatChem*, 2020, **12**, 27–40; (h) R. Francke and R. D. Little, *ChemElectroChem*, 2019, **6**, 4373–4382; (i) P. Xiong and H.-C. Xu, *Acc. Chem. Res.*, 2019, **52**, 3339–3350; (j) T. H. Meyer, L. H. Finger, P. Gandeepan and L. Ackermann, *Trends Chem.*, 2019, **1**, 63–76; (k) A. Wieben, T. Gieshoff, S. Möhle, E. Rodrigo, M. Zirbes and S. R. Waldvogel, *Angew. Chem., Int. Ed.*, 2018, **57**, 5594–5619; (l) S. Tang, Y. Liu and A. Lei, *Chem*, 2018, **4**, 27–45; (m) M. D. Kärkäs, *Chem. Soc. Rev.*, 2018, **47**, 5786–5865; (n) K. D. Moeller, *Chem. Rev.*, 2018, **118**, 4817–4833; (o) N. Sauermann, T. H. Meyer, Y. Qiu and L. Ackermann, *ACS Catal.*, 2018, **8**, 7086–7103; (p) K.-J. Jiao, C. Ma, P. Fang and T.-S. Mei, *ACS Catal.*, 2018, **8**, 7179–7189; (q) N. Sauermann, T. H. Meyer and L. Ackermann, *Eur. J.*

- Chem.*, 2018, **24**, 16209–16217; (r) M. Yan, Y. Kawamata and P. S. Baran, *Chem. Rev.*, 2017, **117**, 13230–13319; (s) A. Jutand, *Chem. Rev.*, 2008, **108**, 2300–2347.
- A. Studer and D. P. Curran, *Nat. Chem.*, 2014, **6**, 765–773.
- (a) Z.-H. Wang, P.-S. Gao, X. Wang, J.-Q. Gao, X.-T. Xu, Z. He, C. Ma and T.-S. Mei, *J. Am. Chem. Soc.*, 2021, **143**, 15599–15605; (b) X. Chang, Q. Zhang and C. Guo, *Angew. Chem., Int. Ed.*, 2020, **59**, 12612–12622; (c) L. Song, N. Fu, B. G. Ernst, W. H. Lee, M. O. Frederick, R. A. DiStasio Jr and S. Lin, *Nat. Chem.*, 2020, **12**, 747–754; (d) H. Qiu, B. Shuai, Y.-Z. Wang, D. Liu, Y.-G. Chen, P.-S. Gao, H.-X. Ma, S. Chen and T.-S. Mei, *J. Am. Chem. Soc.*, 2020, **142**, 9872–9878; (e) P.-S. Gao, X.-J. Weng, Z.-H. Wang, C. Zheng, B. Sun, Z.-H. Chen, S.-L. You and T.-S. Mei, *Angew. Chem., Int. Ed.*, 2020, **59**, 15254–15259; (f) T. J. DeLano and S. E. Reisman, *ACS Catal.*, 2019, **9**, 6751–6754 For representative reviews on asymmetric electrosynthesis and electrocatalysis, see: (g) C. Zhu, N. W. J. Ang, T. H. Meyer, Y. Qiu and L. Ackermann, *ACS Cent. Sci.*, 2021, **7**, 415–431; (h) Q. Lin, L. Li and Z. Luo, *Eur. J. Chem.*, 2019, **25**, 10033–10044; (i) M. Ghosh, V. S. Shinde and M. Rueping, *Beilstein J. Org. Chem.*, 2019, **15**, 2710–2746.
- (a) J. K. Cheng, S.-H. Xiang, S. Li, L. Ye and B. Tan, *Chem. Rev.*, 2021, **121**, 4805–4902; (b) Y.-B. Wang and B. Tan, *Acc. Chem. Res.*, 2018, **51**, 534–547; (c) J. E. Smyth, N. M. Butler and P. A. Keller, *Nat. Prod. Rep.*, 2015, **32**, 1562–1583; (d) E. Kumarasamy, R. Raghunathan, M. P. Sibi and J. Sivaguru, *Chem. Rev.*, 2015, **115**, 11239–11300; (e) D. Parmar, E. Sugiono, S. Raja and M. Rueping, *Chem. Rev.*, 2014, **114**, 9047–9153; (f) J. Yu, F. Shi and L.-Z. Gong, *Acc. Chem. Res.*, 2011, **44**, 1156–1171; (g) G. Bringmann, T. Gulder, T. A. M. Gulder and M. Breuning, *Chem. Rev.*, 2011, **111**, 563–639; (h) M. C. Kozłowski, B. J. Morgan and E. C. Linton, *Chem. Soc. Rev.*, 2009, **38**, 3193–3207; (i) Y. Chen, S. Yekta and A. K. Yudin, *Chem. Rev.*, 2003, **103**, 3155–3212.
- (a) J. K. Cheng, S.-H. Xiang, S. Li, L. Ye and B. Tan, *Chem. Rev.*, 2021, **121**, 4805–4902; (b) B. Zu, Y. Guo, J. Ke and C. He, *Synthesis*, 2021, **53**, 2029–2042; (c) C.-X. Liu, W.-W. Zhang, S.-Y. Yin, Q. Gu and S.-L. You, *J. Am. Chem. Soc.*, 2021, **143**, 14025–14040; (d) J. Wencel-Delord, A. Panossian, F. R. Leroux and F. Colobert, *Chem. Soc. Rev.*, 2015, **44**, 3418–3430.
- I. Takahashi, Y. Suzuki and O. Kitagawa, *Org. Prep. Proced. Int.*, 2014, **46**, 1–23.
- (a) J. Terauchi and D. P. Curran, *Tetrahedron: Asymmetry*, 2003, **14**, 587–592; (b) O. Kitagawa, M. Kohriyama and T. Taguchi, *J. Org. Chem.*, 2002, **67**, 8682–8684.
- (a) L.-P. Chen, J.-F. Chen, Y.-J. Zhang, X.-Y. He, Y.-F. Han, Y.-T. Xiao, G.-F. Lv, X. Lu, F. Teng, Q. Sun and J.-H. Li, *Org. Chem. Front.*, 2021, **8**, 6067–6073; (b) O. Kitagawa, *Acc. Chem. Res.*, 2021, **54**, 719–730; (c) D. Li, S. Wang, S. Ge, S. Dong and X. Feng, *Org. Lett.*, 2020, **22**, 5331–5336; (d) Y. Kikuchi, C. Nakamura, M. Matsuoka, R. Asami and O. Kitagawa, *J. Org. Chem.*, 2019, **84**, 8112–8120; (e) S.-L. Li, C. Yang, Q. Wu, H.-L. Zheng, X. Li and J.-P. Cheng, *J. Am.*



- Chem. Soc.*, 2018, **140**, 12836–12843; (f) Y. Liu, X. Feng and H. Du, *Org. Biomol. Chem.*, 2015, **13**, 125–132; (g) S. Shirakawa, K. Liu and K. Maruoka, *J. Am. Chem. Soc.*, 2012, **134**, 916–919; (h) O. Kitagawa, M. Yoshikawa, H. Tanabe, T. Morita, M. Takahashi, Y. Dobashi and T. Taguchi, *J. Am. Chem. Soc.*, 2006, **128**, 12923–12931.
- 9 K. Tanaka, K. Takeishi and K. Noguchi, *J. Am. Chem. Soc.*, 2006, **128**, 4586–4587.
- 10 (a) D. Wang, Q. Jiang and X. Yang, *Chem. Commun.*, 2020, **56**, 6201–6204; (b) H.-Y. Bai, F.-X. Tan, T.-Q. Liu, G.-D. Zhu, J.-M. Tian, T.-M. Ding, Z.-M. Chen and S.-Y. Zhang, *Nat. Commun.*, 2019, **10**, 3063–3071; (c) S. Brandes, M. Bella, A. Kjærsgaard and K. A. Jørgensen, *Angew. Chem., Int. Ed.*, 2006, **45**, 1147–1151.
- 11 (a) Y.-J. Wu, P.-P. Xie, G. Zhou, Q.-J. Yao, X. Hong and B.-F. Shi, *Chem. Sci.*, 2021, **12**, 9391–9397; (b) Q.-J. Yao, P.-P. Xie, Y.-J. Wu, Y.-L. Feng, M.-Y. Teng, X. Hong and B.-F. Shi, *J. Am. Chem. Soc.*, 2020, **142**, 18266–18276.
- 12 T. H. Meyer, L. H. Finger, P. Gandeepan and L. Ackermann, *Trends Chem.*, 2019, **1**, 63–76.
- 13 (a) U. Dhawa, C. Tian, T. Wdowik, J. C. A. Oliveira, J. Hao and L. Ackermann, *Angew. Chem., Int. Ed.*, 2020, **59**, 13451–13457; (b) U. Dhawa, T. Wdowik, X. Hou, B. Yuan, J. C. A. Oliveira and L. Ackermann, *Chem. Sci.*, 2021, **12**, 14182–14188.
- 14 For detailed information, see the ESI.†
- 15 (a) *Science of Synthesis: Electrochemistry in Organic Synthesis*, ed. L. Ackermann, Thieme, Stuttgart, 2021; (b) R. Francke and R. D. Little, *Chem. Soc. Rev.*, 2014, **43**, 2492–2521.
- 16 (a) T. M. Masson, S. D. A. Zondag, K. P. L. Kuijpers, D. Cambié, M. G. Debije and T. Noël, *ChemSusChem*, 2021, **14**, 5417–5423; (b) T. H. Meyer, G. A. Chesnokov and L. Ackermann, *ChemSusChem*, 2020, **13**, 668–671; (c) B. H. Nguyen, R. J. Perkins, J. A. Smith and K. D. Moeller, *Beilstein J. Org. Chem.*, 2015, **11**, 280–287.
- 17 (a) Z. Fan, K. L. Bay, X. Chen, Z. Zhuang, H. S. Park, K. Yeung, K. N. Houk and J.-Q. Yu, *Angew. Chem., Int. Ed.*, 2020, **59**, 4770–4777; (b) J. Wu, N. Kaplaneris, S. Ni, F. Kaltenhäuser and L. Ackermann, *Chem. Sci.*, 2020, **11**, 6521–6526; (c) I. Funes-Ardoiz and F. Maseras, *Eur. J. Chem.*, 2018, **24**, 12383–12388; (d) K. L. Bay, Y.-F. Yang and K. N. Houk, *J. Organomet. Chem.*, 2018, **864**, 19–25; (e) M. D. Lotz, N. M. Camasso, A. J. Canty and M. S. Sanford, *Organometallics*, 2017, **36**, 165–171.

